agronomy

MDPI

Article

Geochemical Behaviors of Heavy Metal(loid)s in Soil Ferromanganese Nodules in Typical Karst Areas in Southwest China

Wenbing Ji [1,†], Zhixiang Luo [2,†], Jianyu Huang [3], Xu Liu [4], Haiyun He [5], Yang Gong [1], Meng Chen [1], Yubo Wen [6] and Rongrong Ying [1,*]

[1] Nanjing Institute of Environmental Sciences, Ministry of Ecology and Environment, Nanjing 210042, China; 13121531228@163.com (W.J.); gongyang@nies.org (Y.G.); chenmeng@nies.org (M.C.)
[2] Guangxi Product Quality Inspection Institute, Nanning 530007, China; redindary@163.com
[3] Hechi Environmental Emergency and Solid Waste Technology Center, Hechi 547000, China; hchbjjdk@126.com
[4] Chinese Research Academy of Environmental Sciences, Beijing 100012, China; liuxunm@outlook.com
[5] Eco-Environmental Sciences Research & Design Institute of Zhejiang Province, Hangzhou 310007, China; zjhhyun@126.com
[6] School of Geographical Science, Nantong University, Nantong 226000, China; wenyubo@ntu.edu.cn
* Correspondence: yrr@nies.org
† These authors contributed equally to this work.

Abstract: The ferromanganese nodules (FMNs) developing in soils of karst regions are naturally characterized by high heavy metal(loid)s contents due to several geological factors. Soil FMNs can considerably influence the geochemical behaviors of soil heavy metal(loid)s. However, the mechanisms of the FMN effects in soils of karst areas soils remain unclear, resulting in less understanding of the development process of karst soils. Therefore, the present study aims to investigate 21 individual FMNs collected in soils derived from carbonate rocks in Guangxi province, China, to reveal the mechanisms of heavy metal(loid)s enrichment in FMNs. The studied soil FMNs were mainly composed of Fe_2O_3, SiO_2, Al_2O_3, MnO_2, and TiO_2, with proportions of 25.95, 20.8, 19.07, 3.98, and 1.23%, respectively. Compared to the background soils of Guangxi, the soil FMNs exhibited great enrichment in heavy metal(loid)s. The enrichment factors followed the order of Cd (243.33), Cr (49.67), Cu (5.46), Ni (8.37), Pb (23.68), Zn (15.4), and As (20.11). The heavy metal(loid)s contents in the soil FMNs of the karst areas were much higher than those observed in non-karst areas worldwide. According to the principal component analysis (PCA) results, the first three principal components contributed to about 88.81% of the total variance of the FMN compositions. PC1 (50.90%) suggested the presence of quartz, feldspar, and clay minerals-related elements in the soil FMNs, whereas PC2 (27.10%) and PC3 (10.81%) indicated the presence of Mn(oxyhydr)oxides and Fe(oxyhydr)oxides-related elements in the soil FMNs, respectively. The obtained selective extraction results demonstrated that up to 93% of the total contents of heavy metal(loid)s, namely, Cd, Pb, Cu, Ni, and Zn, were bound to Mn(oxyhydr)oxides. In contrast, oxyanionic species (As and Cr) were predominantly sequestered in Fe(oxyhydr)oxides.

Keywords: ferromanganese nodules; heavy metal(loid)s; karst areas; enrichment factors; obtained selective extraction

Citation: Ji, W.; Luo, Z.; Huang, J.; Liu, X.; He, H.; Gong, Y.; Chen, M.; Wen, Y.; Ying, R. Geochemical Behaviors of Heavy Metal(loid)s in Soil Ferromanganese Nodules in Typical Karst Areas in Southwest China. *Agronomy* **2023**, *13*, 1602. https://doi.org/10.3390/agronomy13061602

Academic Editor: Qingling Fu

Received: 8 May 2023
Revised: 7 June 2023
Accepted: 12 June 2023
Published: 13 June 2023

1. Introduction

Migration and enrichment of metal(loid)s in soils subject to seasonal changes in the redox potential (Eh) and pH may lead to the formation of ferromanganese nodules (FMNs) consisting largely of Fe and Mn (oxyhydr)oxides [1–6]. Previous studies have demonstrated the vital role of FMNs in the behavior of heavy metal(loid)s, as they are important sources and sinks of soil heavy metal(loid)s due to their strong adsorption capacities [7–10]. Studying morphology, structure, minerals, and geochemical characteristics of FMNs is, therefore,

of great theoretical and practical importance in exploring the formation and evolution of soils, as well as the fixation, release, and migration of soil heavy metal(loid)s [11–14].

Karst is a general term used to describe some terrains where rocks (e.g., limestone and dolomite) are influenced by the action of water (chemical dissolution), as well as by the mechanical action of water erosion, subduction, and collapse [15]. Karst areas in Southwest China are among the most affected areas by soil heavy metal pollution in China, especially in Guangxi, Guizhou, Yunnan, and Sichuan provinces. According to the Chinese Soil Environmental Quality Standard [16], soil heavy metal contents exceedances in karst areas of Southwest China are closely related to geological processes, unlike other areas, where exogenous inputs are the main sources of soil pollution [17–21]. High geological background-induced soil contamination in karst areas has attracted increasing attention from researchers in recent years [22–24]. The main soil-forming parent materials in karst areas are carbonate rocks, which release large amounts of Ca, Na, Mg, K, and other elements through the weathering processes, while Fe, Al, Mn, and other insoluble elements are greatly enriched in soils of karst areas, forming neo-formed minerals rich in Fe, Al, and Mn [18]. Indeed, high enrichment of these elements in soils leads to the formation of secondary FMNs [14]. FMNs in karst areas are relatively common and have been increasingly investigated by numerous researchers in recent years [24–26]. Previous studies on FMNs in karst areas have mainly focused on the formation mechanisms of FMNs, isotopic fractionation effects, elemental differences in FMNs with different grain sizes, and mineral composition characteristics [13,19–21,25,26]. However, the enrichment mechanisms of heavy metal(loid)s in FMNs are still unclear.

Guangxi is the second largest province in China in terms of karst areas in the southwestern karst region, second only to Guizhou Province, with a total karst area of about 96,372 km^2, accounting for about 40.7% of the total land area of Guangxi province [27]. FMNs are widespread in the soils of karst areas in Guangxi province, showing relatively high proportions in the soils [19]. In addition, large amounts of FMNs were formed during the weathering processes of carbonate rocks to form soils, resulting in strong secondary enrichment of soil heavy metal(loid)s. In fact, previous studies have shown substantially higher heavy metal(loid)s contents in soil FMNs in karst areas than those in non-karst areas [20,21,24]. According to previous studies, the cadmium (Cd) content in soil FMNs in karst areas reached 299.00 mg kg^{-1}, which is substantially higher than that of the Chinese soil background of Cd (0.097 mg kg^{-1}) [13,28]. The accumulation of soil heavy metal(loid)s contents in karst areas is very closely related to the extensive development of FMNs in soils [13]. Selective extraction of soil heavy metal(loid)s can provide better insights into the partitioning of soil trace elements within the major phases of FMNs than those of scanning electron microscope (SEM) and electron probe micro-analyzer (EPMA) observations [6].

Soil FMNs in karst areas can substantially influence the geochemical behavior of soil heavy metal(loid)s [26]. However, the mechanisms underlying the effects of soil FMNs in karst areas remain unclear. Investigating the accumulation of carbonate rock-derived heavy metal(loid)s in FMNs in terra rossa is, therefore, important for understanding the formation processes of FMNs-containing heavy metal(loid)s. In addition, it is of great importance to reveal the mechanisms constraining the geochemical behavior of heavy metal(loid)s by FMNs in soils in karst areas to ensure reliable land use and planning in high geological background areas. In this study, a typical karst Guangxi area was selected to investigate soil FMNs, thus deepening the understanding of the geochemical mechanisms of enrichment and migration of soil heavy metal(loid)s during the epigenesis process. The present study aims to: (1) reveal the mechanisms of heavy metal(loid)s enrichment in soil FMNs of karst areas in Guangxi Province using targeted extraction experiments of FMNs and principal component analysis; and (2) identify the main factors affecting the accumulation of heavy metal(loid)s in soil FMNs.

2. Materials and Methods

2.1. Study Area

Guangxi Province is located in South China between latitude and longitude ranges of 20°54′~26°24′ N and 104°26′~112°04′ E, respectively, with an elevation range of 50–200 m. The Tropic of Cancer crosses the central part of Guangxi Province. The study area is characterized by a subtropical monsoon climate zone, with average annual temperature and average annual rainfall ranges of 16.5–23.1 °C and 1077.4–2768.8 mm, respectively [23]. Most of the region is characterized by a warm climate, abundant rainfall, and distinct dry and wet seasons. The parent rocks consist primarily of carbonates, siliciclastic, clastic, and Quaternary sediments. Carbonate rocks are mainly distributed in the north-central and southwestern parts of the region, with a geological background of Carboniferous-Permian and Devonian strata, respectively [26]. The study area is located in the central region of Guangxi province in the typical karst development areas of Nanning, Guigang, and Chongzuo cities, where soil FMNs are prevalent. The main soil types in the study area are Ferralsols, Luvisols, Cambisols, and Anthrosols.

2.2. Soil Sample Collection and Preparation

In this study, surface soil samples were collected from the 0–20 cm soil layer to obtain FMNs from the FMN development area. Soil samples were collected from 5 sub-sample points and mixed to obtain a composite sample. The sampling sites were mainly located in Nanning, Guigang, and Chongzuo cities (Figure 1). In addition, a total of 21 FMN samples were collected following the Land Quality Geochemical Assessment Specification [29]. The size of FMN samples mainly range from 1 to 4 mm. The collected soil samples were first washed with deionized water to remove soil particles adhering to the surface of FMNs, then dried at room temperature (25 °C). Well-developed FMNs were hand-selected, placed in clean self-sealing bags, and sent to the laboratory for analysis. The FMN samples were individually ground to a fine powder using an agate mortar and stored in a dry place for further analysis [21,25,26].

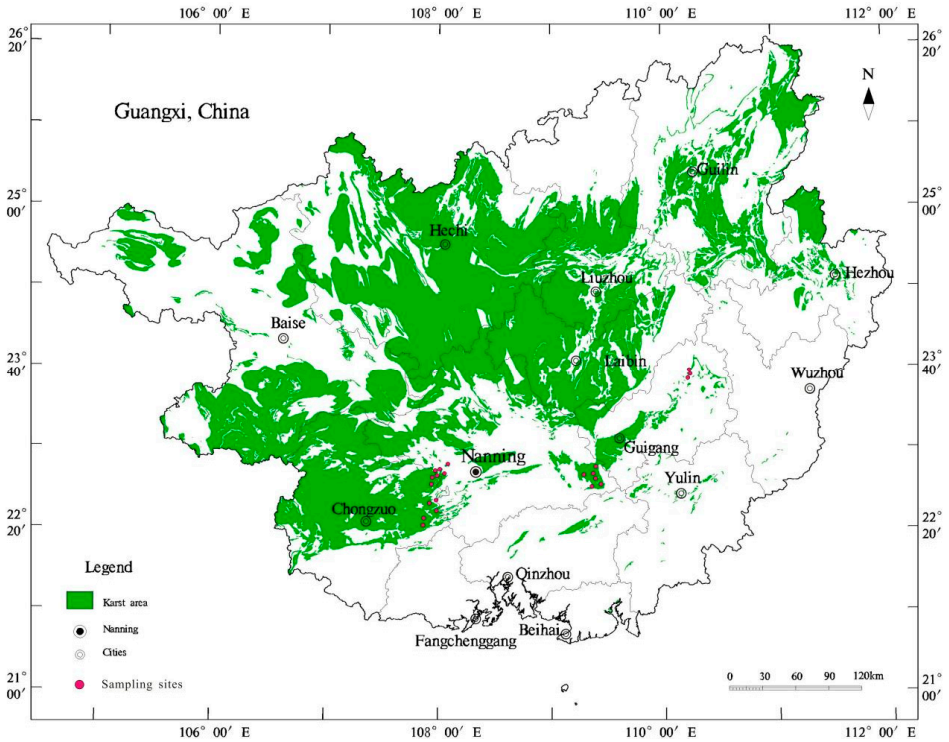

Figure 1. Sampling sites in the study area.

2.3. Chemical Analysis

In this study, the Al_2O_3, CaO, Fe_2O_3, K_2O, MgO, Na_2O, SiO_2, TiO_2, and P_2O_5 concentrations were determined using X-ray fluorescence spectroscopy (XRF, ARL9900, Thermo Fisher Scientific, Waltham, MA, USA). The Mn and Cu concentrations were analyzed using inductively coupled plasma atomic emission spectroscopy (ICP-AES, iCAP 7400, Thermo Fisher, USA), while the As concentrations were determined by atomic fluorescence spectrophotometry (AFS, Model AFS-230E; Kechuang Haiguang Instrument Co., Ltd., Beijing, China). In addition, the Pb, Cr, Zn Cd, and Ni concentrations were analyzed using inductively coupled plasma mass spectrometry (ICP-MS, iCAP RQ Thermo Fisher, USA). Analytical accuracy and precision were determined based on standard reference materials (GSS17, GSS22, GSS25, and GSS27). The relative double difference (RD, %) was calculated in this study to control data quality. The relative standard deviations of the analysis results were below 10%.

2.4. Selective Extractions

In order to further investigate the interrelationship of different of heavy metal(loid)s of each component of FMNs, typical FMNs were selected for selective extraction experiments. Selective extractions of the major and trace elements can provide further insights into the distribution and partitioning of heavy metal(loid)s in the different mineral phases of soil FMNs.

To understand the interrelationship between different heavy metal(loid)s in each component of FMNs in the study area, the following selective extraction methods were used in this study [8]. (1) Control experiments were conducted in this section. An amount of 100 mL of 0.5 mol/L HNO_3 was first added to 100 mg of the FMN power sample, which was then stirred for 30 min at 5000 rpm and room temperature until thorough mixing was achieved. The solution was centrifuged before collecting the supernatant to determine the elemental contents, with a solid-to-liquid ratio of 100 mg/100 mL. (2) An amount of 100 mg of the FMN powder sample was added to 200 mL of 0.1 mol/L of NH_2OH-HCl (non-acidified), with a pH value of 3.6, which was then stirred for 2 h at room temperature. The supernatant was collected after sufficient reaction, and then it was centrifuged and analyzed for the Al, Fe, Mn, As, Cd, Cr, Cu, Ni, Pb, and Zn contents. (3) An amount of 100 mg of the FMN powder sample was added to a solution containing 50 mL of 30% H_2O_2 and 50 mL of 1 mol/L HNO_3 (solid/extractant ratio of 100 mg/100 mL), which was then stirred at room temperature stirring for 30 min. Afterward, the solution was centrifuged before collecting the supernatant and analyzed for those elements. (4) The solid sample was extracted from a 100 mg FMN powder sample using 40 mL of 0.3 mol/L sodium citrate ($Na_3C_6H_5O_7$-$2H_2O$); then, 5 mL of 1 mol/L sodium bicarbonate ($NaHCO_3$) and 1 g of sodium dithionite ($Na_2S_2O_4$) were stirred in a water bath at 80 °C for 1 h. These solutions were added to the FMN powder sample. After thorough mixing was achieved, the supernatant was centrifuged, and then it was collected and analyzed for those elements. The filtered solutions in each extraction step were analyzed using ICP-MS. The data quality control was assessed by comparing the measured contents in standard substances (SS2001, SS3001, and SS4001) with those revealed in the FMN powder sample. The ratio of the actual results to the results of the standard substances ranged from 80 to 120%, indicating the reliable quality of the results.

2.5. Statistical Analysis

In this study, descriptive statistics, Pearson's correlation analysis, and principal component analysis were performed using SPSS (version 24, IBM SPSS Statistics) to assess the relationships between the major and heavy metal(loid)s. In addition, geographical distribution maps were generated using ESRI-Arc GIS geospatial software (version 10.2). Multivariate statistical methods can be used to assess the potential relationships between numerous variables through a comprehensive analysis of multiple factors. Indeed, several related studies have applied multivariate statistical methods to determine the potential

sources of soil heavy metal(loid)s pollution. Among them, Principal Component Analysis (PCA) can simultaneously reveal the variables that contribute the most to the variance. In addition, PCA can be used to explore the relationships between different variables and determine their contributions to the explained variance [30]. In this study, a PCA was performed for the macronutrient and trace elements of the collected FMNs from the karst areas of Guangxi province.

3. Results and Discussion

3.1. Elemental Concentrations

3.1.1. Major Element Concentrations

According to the obtained results, FMNs mainly contained five elements, namely, Fe_2O_3 (24.56%), SiO_2 (23.17%), Al_2O_3 (18.75%), MnO_2 (4.20%), and TiO_2 (1.22%), with an average content greater than 1% (Table 1). The sum proportion of the five elements was 71.9%. It should be noted that the proportions of alkaline earth elements were all lower than 1%. The average contents of CaO, MgO, K_2O, and Na_2O were 0.70, 0.39, 0.38, and 0.06%, respectively, while the average proportion of P_2O_5 was 0.94%. The elemental composition characteristics in the present study area were similar to those observed in FMNs in other karst areas in China [26]. In contrast, the obtained results revealed considerable differences between the elemental compositions of the soil FMNs in this study and those observed in other areas worldwide, including Indiana in the United States [31], Sicily in Italy [32], and China [11]. Indeed, the major elemental compositions in the 1–2 mm FMNs in Indiana, USA, followed the order of SiO_2 (55.27%) > Fe_2O_3 (30.94%) > Al_2O_3 (8.92%) > MnO_2 (1.59%) > K_2O (1.09%), while those in the 1–2 mm FMNs followed the order of SiO_2 (61.60%) > Fe_2O_3 (25.28%) > Al_2O_3 (8.44%) > K_2O (1.19%) > MnO_2 (1.15%) [31]. Neaman et al. [8] reported that the average compositions of soil FMNs in Serra do Navio in Brazil followed the order of Fe_2O_3 (41.88%) > MnO_2 (15.93%) > SiO_2 (14.67%) > Al_2O_3 (12.55%), whereas Palumbo et al. [32] reported that the average compositions of soil FMNs in Sicily, Italy, followed the order of Al_2O_3 (13.27%) > Fe_2O_3 (12.26%) > MnO_2 (6.54%) > K_2O (1.24%). Although the studied soil FMNs showed great variations in the compositions between regions worldwide, they predominately contain Fe, Mn, Si, and Al. The study area is characterized by strong chemical weathering during the epigenetic processes due to the high average air temperatures and abundant rainfall [21,26].

Compared with the soil background values of Guangxi, the enrichment factors of the major six elements followed the order of MnO_2 (132.65) > Fe_2O_3 (7.15) > P_2O_5 (6.72) > CaO (4.12) > TiO_2 (2.2) > Al_2O_3 (1.46). In contrast, four elements showed relatively low enrichment factors, according to the order of MgO (0.89) > Na_2O (0.65) > K_2O (0.34) > SiO_2 (0.28) (Table 1). The solubility of Fe, Al, Mn, and Ti in water are relatively low. In addition, the rock weathering process can lead to the migration of highly soluble elements (e.g., Mg, K, and Na) into water bodies, explaining the low average proportions of K_2O, MgO, and Na_2O in the soil FMNs of less than 1%. This finding reflects the actual status of soil FMNs in the subtropical environment of Guangxi province, with a high temperature and humidity environment, due to the strong weathering and leaching effects, thereby substantially decreasing the contents of these elements in soil FMNs following the weathering process of rocks [26]. Some degree of calcium (Ca) enrichment in FMNs might occur in the study area as calcium carbonate ($CaCO_3$) was not completely weathered after the formation of FMNs, remaining relatively stable in FMNs. In addition, some other minerals (e.g., lithiophorite, goethite, and quartz) closely related to the major elements can be identified in FMNs [20].

Table 1. Concentrations of major elements in FMNs, soils, and the average upper crustal composition (AUCC) (%).

Samples	Al_2O_3	SiO_2	Fe_2O_3	MnO_2	K_2O	Na_2O	CaO	MgO	P_2O_5	TiO_2	References
FMNs (n = 21)	18.75 ± 1.86 (14.39–22.04)	23.17 ± 6.34 (13.63-36.41)	24.56 ± 4.64 (15.17–31.57)	4.2 ± 3.59 (0.51–12.40)	0.54 ± 0.41 (0.15–1.31)	0.06 ± 0.01 (0.048–0.081)	0.83 ± 0.97 (0.16–2.95)	0.47 ± 0.19 (0.25–0.78)	0.81 ± 0.35 (0.34–1.41)	1.22 ± 0.19 (0.95–1.62)	This study
FMNs (1–2 mm) in Indiana loess	8.92	55.27	30.94	1.59	1.09	0.46	0.22	0.52	0.3	0.77	[31]
FMNs (0.5–1 mm) in Indiana loess	8.44	61.6	25.28	1.15	1.19	0.51	0.26	0.53	0.29	0.75	[31]
Nine kinds of FMNs in China	12.35	43.2	13.77	12.21	0.46	0.12	0.89	0.92	0.11	0.72	[11]
FMNs in Sicilian soils, Italy	13.267	/	12.262	6.542	1.241	0.188	0.392	0.592	/	/	[32]
FMNs in red soils in Guangxi	17.93	19.72	30.06	0.64	0.12	0.05	0.13	0.21	0.78	0.96	[20]
Iron nodules (n = 26)	19.53	18.42	2.71	1.09	0.1	0.05	0.12	0.19	0.83	0.97	[21]
Manganese nodules (n = 21)	17.12	25.09	18.51	10.36	0.79	0.07	1.16	0.6	0.52	1.33	[13]
Nodules	12.55	14.67	41.88	15.93	0.32	nd	nd	0.22	0.32	1.11	[7]
Nodules (n = 53) in Guangxi	16.10	23.97	27.71	7.44	0.47	0.09	0.71	0.58	-	-	[26]
Lateritic subsoil in Serra do Navio of Brazil	27.98	31.94	18.36	1.12	0.17	nd	nd	0.2	0.14	2.59	[8]
AUCC	15.4	66.62	5.6	0.12	2.8	3.27	3.59	2.48	1.49	0.64	[33]
Background soil (China)	13.62	63.94	4.64	0.1	2.4	1.28	2.9	1.5	0.11	0.53	[34]
Background soil (Guangxi)	13.07	73.67	3.63	0.03	1.12	0.09	0.17	0.44	0.14	0.56	[35]
* Enrichment factors	1.46	0.28	7.15	132.65	0.34	0.65	4.12	0.89	6.72	2.20	

* Enrichment factors = calculated as the ratio of the element concentration in the nodules to that of the background soil of Guangxi [12].

Manganese (Mn) and iron (Fe) can exhibit different valence states, of which elements with higher and lower valence states are prone to precipitate and dissolve, respectively [10]. Soil Mn and Fe are often present in the forms of Mn^{2+}, Mn^{3+}, Mn^{4+}, Fe^{2+}, and Fe^{3+}. In addition, the interconversion of the Fe and Mn oxidation states is influenced mainly by pH, redox potential (Eh), and microbial activity of the soil environment [11]. The main mineral compositions of soil FMNs in karst areas consisted of quartz, goethite, clinochlore, illite, kaolinite, boehmite, albite, microcline, lithiophorite, and hematite [20].

Goethite and hematite consist mainly of Fe oxides. Contrary to goethite which is widely distributed regardless of climate and region, hematite can only form under specific environmental conditions [10]. The identified Mn minerals in soil FMNs in Guangxi are birnessite, vernadite, lithiophorite, manganite, and coronadite [20]. FMN phosphorus (P) in the form of PO_4^{3-} can be adsorbed on the surface of Fe oxides to form a complex anion group without forming particular minerals [4,10]. In this study, the proportion of TiO_2 in FMNs was higher than 1%, which might be related to the formation of rutile in FMNs [31].

Al and Si are relatively stable during epigenesis [23]. However, weathering of primary minerals (e.g., feldspar) can release Al and Si and, consequently, enrich clay minerals, such as kaolinite, illite, vermiculite, and montmorillonite. On the other hand, Si can be stable in the soil and new-formed FMNs for a long time in the form of quartz (SiO_2) particles.

3.1.2. Heavy Metal(loid)s Concentrations

Compared with the soil background values of Guangxi province, the heavy metal(loid)s enrichment values in FMNs were Cd (243.33), Cr (49.67), Cu (5.46), Ni (8.37), Pb (23.68), Zn (15.4), and As (20.11) (Table 2). Guangxi is a typical karst region where heavy metal(loid)s may be substantially enriched in the soil due to the weathering process of soil-forming parent rocks. The weathering-induced FMNs can, therefore, be strongly enriched in heavy metal(loid)s. According to Wen et al. [18], the Cd contents in the karst region of Guangxi followed the order of carbonate rocks (0.45 mg kg^{-1}) < saprolite (4.41 mg kg^{-1}) < terra rossa (4.94 mg kg^{-1}) < Fe–Mn concretion (37.5 mg kg^{-1}). The heavy metal(loid)s contents in FMNs were substantially higher than the average heavy metal(loid)s contents in the upper continental crust (AUCC), as well as in soils in China and worldwide (Table 2). The enrichment of soil FMNs in other regions worldwide may exhibit large regional variations (Table 2). However, the average heavy metal(loid)s contents in the soil FMNs of karst areas were higher than those in non-karst regions except Cu and Pb (Table 2).

3.2. Relationships between Major and Trace Elements in FMNs

The geochemical behavior of heavy metal(loid)s (Cd, Cr, Pb, As, Cu, Ni, and Zn) is mainly controlled by the major oxides (Al_2O_3, CaO, Fe_2O_3, K_2O, MgO, Na_2O, SiO_2, TiO_2, and P_2O_5). The obtained PCA results are reported in Table 3. The cumulative contribution of the first three principal components (PC1, PC2, and PC3) was 88.81% (Table 3). The larger the eigenvalue of the principal component (PC), the higher the contribution to the explained variance.

Table 2. Concentrations of heavy metal(loid)s in FMNs, soils, and AUCC (mg kg^{-1}).

Samples	Cd	Cr	Cu	Ni	Pb	Zn	As	References
Fe–Mn nodules (*n* = 21)	35.04 ± 26.58 (8.91–99.9)	2483.29 ± 1491.7 (392–5180)	98.34 ± 25.77 (55.7–149)	125.51 ± 38.06 (74–209)	568.33 ± 276.62 (274–1148)	662 ± 190.32 (323–905)	160.9 ± 24.97 (116–208)	This study
Fe–Mn nodules (*n* = 15) in Guangxi of China	71.59	968.89	101.52	163.84	947.13	637.07	NA [b]	[19]
Terra rossa (*n* = 308) in Guangxi of China	1.49	194	37.2	42.6	58.6	159	NA [b]	[18]
Fe–Mn nodules (*n* = 20) in Guangxi of China	37.5	573	84.9	129	461	641	NA [b]	[18]
Background soil (China)	0.097	61	22.6	26.9	26	74.2	11.2	[28]
Fe–Mn nodules in the northern part of Namibia	6.83	36.1	447	89.6	597	137	23.1	[6]
Fe–Mn nodules (*n* = 18) from Sicilian soils, Italy	22.50	NA [b]	63.72	249.78	558	108.17	NA [b]	[32]
Fe–Mn nodules (*n* = 9) in main soils of China	9.54	41.5	152.3	282.6	4622	411.9	NA [b]	[11]
Fe–Mn nodules (*n* = 4) in Quaternary red earth of Eastern China	0.02	NA [b]	56.70	160.43	2875	103.34	NA [b]	[12]
Fe–Mn nodules (*n* = 7) in Guangxi of China	3.76	627	59	153	90.8	603	39.5	[24]
World soil	0.35	40	30	20	19	90	NA [b]	[36]
AUCC	0.00009	92	28	47	17	67	4.8	[33]
Background soil (Guangxi)	0.144	50	18	15	24	43	8	[35]
Enrichment factors [a]	243.33	49.67	5.46	8.37	23.68	15.40	20.11	

[a] Enrichment factor = calculated as ratio of element concentrations in the nodules to that in the background soil in Guangxi [12]. [b] NA: not available.

Table 3. Maximum variance rotation matrix of FMNs.

Properties	PC1	PC2	PC3
Al_2O_3	−0.517	−0.265	0.636
SiO_2	0.813	0.167	−0.183
Fe_2O_3	−0.780	−0.503	0.565
MnO_2	0.477	0.821	−0.177
K_2O	0.965	0.183	−0.165
Na_2O	0.841	0.500	−0.129
CaO	0.303	−0.058	−0.930
MgO	0.918	0.178	−0.323
P_2O_5	−0.714	−0.261	0.593
TiO_2	0.128	0.822	0.199
Cd	0.101	0.975	−0.122
Cr	−0.489	−0.639	0.428
Cu	−0.567	0.651	0.403
Ni	0.130	0.809	0.523
Pb	0.301	0.938	0.012
Zn	−0.031	0.372	0.917
As	0.665	−0.168	0.408

The principal components (PC1, PC2, and PC3) explained 88.81% of the variable values of FMNs (Table 3). PC1 contributed to about 50.90% of the total variance, showing high positive loadings on SiO_2, K_2O, Na_2O, MgO, and CaO, which have the highest scores on PC1, showing elements related to clay minerals, quartz, and feldspar. PC2 contributed about 27.10%, showing the high positive loadings on MnO_2, Na_2O, TiO_2, Cd, Cu, Ni, Pb, and Zn, suggesting the presence of Mn(oxyhydr)oxides in soil FMNs (Figure 2). On the other hand, Mn showed significant positive correlation coefficients ($p < 0.01$) with Cd, Cu, and Ni of 0.86, 0.94, and 0.63, respectively, further demonstrating the key contributions of the Mn-containing oxides to the explained variance of PC2 (Figure 2). Although Mn-containing oxides were not abundant in FMNs, showing a lower average proportion than those of Fe, Si, and Al of 3.98%, they have a strong ability to adsorb trace elements due to their special spatial tunneling and layered structure [6]. Manganese minerals can also be effective materials for the remediation and treatment of heavy metal-contaminated soils [37].

FMNs often contain less crystalline Mn(oxyhydr)oxides, such as hydromanganite, chalcocite, and lithiophorite [38–40]. Divalent cations with six coordination sites (Cd^{2+}, Cu^{2+}, Ni^{2+}, Pb^{2+}, and Zn^{2+}) can undergo homogeneous substitution due to their close crystal chemistry. In addition, the negatively charged surfaces of FMNs can enhance the electrostatic and specific adsorption of heavy metal(loid)s cations in the soil solutions [10]. FMNs are usually enriched in trace elements, especially heavy metal(loid)s, compared to the corresponding soils [32,41–44]. However, the enrichment of heavy metal(loid)s in FMNs can vary considerably compared to the corresponding soils. According to Feng et al. [45], the adsorption capacities of Mn-bearing minerals for heavy metal(loid)s (Cd, Co, Cu, Pb, and Zn) followed the order of birnessite >> todorokite ≈ cryptomelane > hausmannite. Hausmannite and manganite can adsorb large amounts of Cd and Co compared to goethite and hematite [46]. In a previous study, the adsorbed divalent trace heavy elements by FMNs followed the order of Pb ≈ Cu > Zn > Co > Ni > Cd, which is consistent with the order of the first hydrolysis constant (*Kh*) of these elements [47]. This finding indicates that Cd is the least adsorbed element by FMNs compared to the other heavy metal(loid)s. However, the adsorbed Cd contents by FMNs may be considered high due to the low Cd background value. Manceau et al. [48] highlighted the substitution of Mn(oxyhydr)oxides-derived Mn^{3+} with Ni in FMNs, producing a homogeneous substitution in the mineral network.

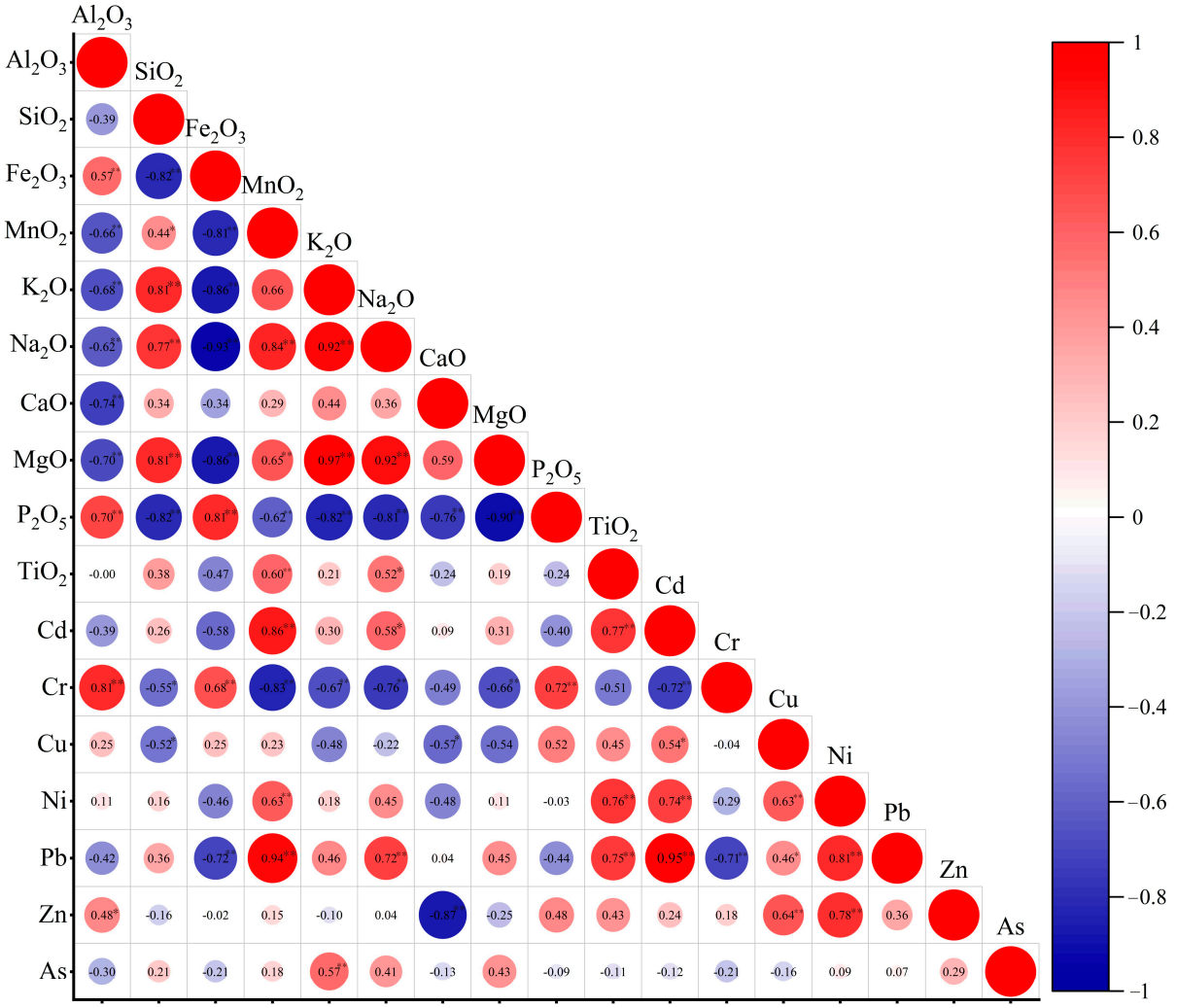

Figure 2. Correlation between heavy metal(loid)s and major elements in FMNs. *: $p < 0.05$; ** $p < 0.01$.

PC3 contributed to about 10.81% of the total variance and showed high positive loadings on Al_2O_3, P_2O_5, Fe_2O_3, Cr, Ni, Zn, and As, showing elements related to Fe(oxyhydr)oxides. Iron is one of the principal elements in rocks and soils, making it the most abundant element in the Earth's crust [33]. Fe(oxyhydr)oxides can influence greatly the formation of FMNs due to their special metastable properties [12,20]. The surfaces of Fe-containing oxides and hydroxides in soils are positively charged, thereby exhibiting strong adsorption effects on cluster anions (e.g., As, Cr, and P). The majority of Fe(oxyhydr)oxides in FMNs are in the mineral form [10]. Gasparatos et al. [3] revealed an Fe proportion range in FMNs of 14.98–16.53%, with an average proportion of 15.96% and an Fe proportion in iron-bearing minerals of 78%. The iron-bearing minerals in FMNs consist generally of goethite (α-FeOOH) and hematite (Fe_2O_3). Arsenic is a naturally occurring toxic element, of which toxicity, mobility, and bioavailability in soils are closely related to the soil pH and redox potential characteristics [21]. Arsenite (AsO_3^{3-}) and arsenate ($H_2AsO_4^-$ and $HAsO_4^{2-}$) are the two main As species present in soils and can usually be adsorbed by Fe oxide films [49]. In contrast, Manceau et al. [50] analyzed As contents in soil FMNs in Morvan, France, using synchrotron-based X-ray microfluorescence (μSXRF) spectroscopy and highlighted strong correlations between As and Fe, with similar spatial As/Fe ratios of the FMNs, indicating a strong association between Fe and As in FMNs. Aide [49] also found a strong positive linear relationship between Cr and Fe contents in FMNs of two poorly drained soil types, with a significant determination coefficient of R^2 of 0.81 ($p < 0.01$) and indicated the substitution of the monocrystalline Cr^{3+} with Fe(oxyhydr)oxides, resulting in strong adsorptions of Cr

forms (e.g., CrO_2^-, $Cr_2O_4^{2-}$, and $Cr_2O_7^{2-}$). Tzou et al. [51] indicated the crucial role of the Fe(oxyhydr)oxide surfaces in Cr adsorption, demonstrating the use of Fe(oxyhydr)oxides in the remediation of Cr-contaminated soils. Manceau et al. [52] used the extended X-ray absorption fine structure (EXAFS) to analyze Ni and Zn contents in FMNs, showing the presence of Ni in goethite and lithiophorite and Zn in goethite, lithiophorite, layered silicate minerals, and birnessite.

3.3. Heavy Metal(loid)s Bindings during the FMN Formation Process

The heavy metal(loid)s content (<0.1%) in FMNs was poorly detected using field emission scanning electron microscopy (FESEM). However, it should be noted that selective extraction experiments often exhibit good trace element distribution results [6,7].

The solubility of different heavy metal(loid)s in blank experiments was generally low in this study (below 5%). The acidified hydrogen peroxide (H_2O_2 + HNO_3) and hydroxylamine hydrochloride (NH_2OH-HCl) were highly selective for Mn oxides, extracting 88.2 and 92.6% of Mn, respectively (Table 4). On the other hand, citric acid-bicarbonate-sodium hyposulfite (CBD) extracted 67.1 and 91.3% of Fe and Mn, respectively, indicating that Fe oxides (hydroxides) (e.g., goethite and hematite) are less soluble than Mn oxides (e.g., lithiophorite) under the same analytical conditions. In control experiments, low acid concentrations resulted in low proportions of dissolved Mn (2.2%), Al (2.5%), and Fe (1.4%), whereas non-crystalline Mn-containing oxides (hydroxides) (e.g., lithiophorite) were combined with large proportions of Cd (86.6–93.2%), Cu (61.7–72.6%), Ni (58.3–66.8%), Pb (42.5–93%), and Zn (47.8–62.3%). In contrast, amorphous Fe oxides (hydroxides) (e.g., goethite and hematite) incorporated most of the As and Cr contents that are generally considered to exist in the form of Fe oxides (hydroxides) [7].

Table 4. Dissolution of selected major and heavy metal(loid)s from FMNs during selective extractions.

Elements	Dissolved (% of the Total)			
	Control (HNO_3) [a]	NH_2OH–HCl	H_2O_2 + HNO_3	CBD
Al	2.5	3.9	14.1	16.6
Fe	1.4	4.8	7.5	67.1
Mn	2.2	88.2	92.6	91.3
As	2.5	4.1	16.5	51.4
Cd	9.3	86.6	93.2	92.6
Cr	0.5	9.5	7.3	48.4
Cu	5.2	61.7	72.6	68.1
Ni	2.1	58.3	66.8	71.9
Pb	2.2	42.5	93.0	89.5
Zn	4.5	47.8	62.3	71.4

[a] Control: 0.5 mol L^{-1} HNO_3; hydroxylamine hydrochloride (NH_2OH-HCl) and acidified hydrogen peroxide (H_2O_2 + HNO_3) targeting Mn (oxyhydr)oxides and Na-citrate-bicarbonate-dithionite (CBD) targeting both Fe and Mn (oxyhydr)oxides.

The adsorption of heavy elements can occur during the entire complex FMN formation process [6,53,54]. Although there are significant differences in the morphology, chemical composition, and mineral composition of soil FMNs between different regions of the world, the conditions necessary for soil FMN formation are similar [31,54,55]. The development of soil FMNs requires at least three conditions: (1) adequate supply of Fe and Mn (oxyhydr)oxides; (2) regular changes in oxidizing and reducing conditions; (3) suitable temperature and sufficient organic carbon contents to support microbial activities.

Many researchers have divided the weathering process of carbonate rocks into two stages, namely, the dissolution/accumulation of insoluble residues in carbonate rocks and the formation of insoluble residues in soils [56,57]. The formation of insoluble residues in soils is similar to the weathering process of non-carbonate rocks (e.g., silicate minerals) [58].

The FMN formation in karst areas is the second stage of residual soil evolution, generally occurring after the weathering process of parent materials and rocks in the soil

formation process [14]. This assumption is, indeed, in line with the high chemical index of alteration (CIA) of soil FMNs in karst areas and the evolutionary trends of different material types in high geological background areas [18]. Soil FMNs in the studied karst areas of Guangxi Province were formed gradually in the second stage, representing the product of the late stage of soil development.

During carbonate rock weathering, large amounts of highly soluble mineral elements (e.g., K, Na, Ca, and Mg) can easily be released through water infiltration and runoff, while less soluble mineral elements (e.g., Fe, Mn, Si, and Al) can eventually accumulate in soils [14,56]. Fe and Mn contents are relatively low and high in carbonate rocks and soils in karst areas, respectively [18,59]. FMNs contain high contents of carbonate protolith-derived heavy metal(loid)s, including Zn, Cu, Cd, Ni, Ba, Pb, and As, involved in the formation process of FMNs [19].

The formation of soil FMNs requires periodic wetting and drought conditions that can lead to periodic changes in redox conditions [6]. Guangxi Province is characterized by a subtropical monsoon climate. In addition, high rainfall amounts occur in the study area in summer, resulting in waterlogging conditions in the soil surfaces of karst areas due to poor drainage, thereby leading to the formation of local reducing environments [14]. Indeed, some researchers have revealed the presence of FMNs in poorly drained soils in the Carpathian Foothills in Poland due to the flooding-induced low oxygen permeability, thus decreasing the Eh values of soils and, consequently, resulting in reducing conditions of the soil environment [42].

In this study, selective extractions provided further insights into the partitioning of heavy metal(loid)s in separate FMN phases. Our results indicated that Mn (oxyhydr)oxides mainly sequestered Cd, Cu, Ni, Pb, and Zn. This finding is consistent with the selective binding of these elements to Mn(oxyhydr)oxides reported in previous studies [6]. In addition, Cd, Cu, Ni, Pb, and Zn were also positively correlated with Fe(oxyhydr)oxides and partly bound to Fe(oxyhydr)oxides of variable crystallinity [6–9,24]. In contrast, our observations confirmed that oxyanionic species (e.g., As and Cr) were predominantly associated with Fe(oxyhydr)oxides, which is in line with the results reported in previous studies (Table 4) [7,9]. These contrasting behaviors of cationic and anionic heavy metal(loid)s might also be related to the differences in their binding to the differently charged surfaces of Mn and Fe(oxyhydr)oxides [53]. Manganese (oxyhydr)oxides can generally exhibit low point of zero charge (pHzpc) values (e.g., $pHzpc_{birnessite}$ = 1.5–2.8) [60]. In addition, the negatively charged surfaces of these oxides preferentially adsorb cationic species, whereas Fe (oxyhydr)oxides can exhibit higher pHzpc values (e.g., $pHzpc_{goethite}$ and $pHzpc_{ferrihydrite}$ are in the range of ~6–9) [60], with predominantly positive surface charges suitable for binding oxyanions, especially under acidic and near-neutral conditions.

4. Conclusions

In this study, the chemical compositions of 21 carbonate-rock-derived soil FMNs in Guangxi province were investigated to reveal the enrichment mechanisms of heavy metal(loid)s in FMNs. The special soil parent material and seasonal changes in the redox and pH conditions induced by the special climatic conditions in the karst study area provide suitable conditions for the formation of soil FMNs. In addition, the studied soil FMNs exhibited high heavy metal(loid)s contents compared to the background soil heavy metal(loid)s values of Guangxi province. The enrichment factors of heavy metal(loid)s followed the order of Cd (243.33) > Cr (49.67) > Pb (23.68) > As (20.11) > Zn (15.4) > Ni (8.37) > Cu (5.46). The heavy metal(loid)s contents in the soil FMNs of the karst areas were much higher than those observed in non-karst areas worldwide. On the other hand, the first three principal components of the PCA explained 88.81% of the total variance of the FMN heavy metal(loid)s. PC1 (50.90%) demonstrated the presence of quartz, feldspar, and clay minerals-related elements in the soil FMNs. However, PC2 (27.10%) and PC3 (10.81%) were mainly related to the presence of Mn(oxyhydr)oxides and Fe(oxyhydr)oxides-related elements in the soil FMNs. The obtained selective extraction results demonstrated that

up to 93% of the total heavy metal(loid)s contents (Cd, Pb, Cu, Ni, and Zn) were bound to Mn(oxyhydr)oxides. In contrast, oxyanionic species (As and Cr) were predominantly sequestered in Fe (oxyhydr)oxides of the soil FMNs.

Author Contributions: W.J.: conceptualization, investigation, visualization, writing—original draft, writing—review and editing; Z.L.: conceptualization, investigation, visualization, writing—original draft, writing—review and editing; J.H.: conceptualization, investigation, visualization, writing—review and editing; X.L., H.H., Y.G. and M.C.: methodology, investigation; Y.W.: funding acquisition, supervision; R.Y.: project administration, funding acquisition, supervision, writing—review and editing. All authors have read and agreed to the published version of the manuscript.

Funding: This study was financially supported by the National Natural Science Foundation of China (No.42207236) and Nantong Basic Science Project (JC12022075).

Conflicts of Interest: The authors declare that they have no known competing financial interests or personal relationships that could have influenced the work reported in this paper.

References

1. Dixon, J.; Skinner, H. Manganese minerals in surface environments. *Catena Suppl.* **1992**, *21*, 31–50.
2. Gasparatos, D.; Tarenidis, D.; Haidouti, C.; Oikonomou, G. Microscopic structure of soil Fe-Mn nodules: Environmental implication. *Environ. Chem. Lett.* **2005**, *2*, 175–178. [CrossRef]
3. Gasparatos, D.; Haidouti, C.; Tarenidis, D. Characterization of iron oxides in Fe-rich concretions from an imperfectly-drained Greek soil: A study by selective dissolution techniques and X-ray diffraction. *Arch. Agron. Soil Sci.* **2004**, *50*, 485–493. [CrossRef]
4. Gasparatos, D. Sequestration of heavy metals from soil with Fe-Mn concretions and nodules. *Environ. Chem. Lett.* **2013**, *11*, 1–9. [CrossRef]
5. Ettler, V.; Tomášová, Z.; Komárek, M.; Mihaljevič, M.; Šebek, O.; Michálková, Z. The pH dependent long-term stability of amorphous manganese oxide in smelter—Polluted soils: Implication for chemical stabilization of metals and metalloids. *J. Hazard. Mater.* **2015**, *286*, 386–394. [CrossRef]
6. Ettler, V.; Chren, M.; Mihaljevič, M.; Drahota, P.; Kříbek, B.; Veselovský, F.; Sracek, O.; Vaněk, A.; Penížek, V.; Komárek, M.; et al. Characterization of Fe-Mn concentric nodules from Luvisol irrigated by mine water in a semi-arid agricultural area. *Geoderma* **2017**, *299*, 32–42. [CrossRef]
7. Neaman, A.; Mouélé, F.; Trolard, F.; Bourrié, G. Improved methods for selective dissolution of Mn oxides: Applications for studying trace element associations. *Appl. Geochem* **2004**, *19*, 973–979. [CrossRef]
8. Neaman, A.; Waller, B.; Mouélé, F.; Trolard, F.; Bourrié, G. Improved methods for selective dissolution of manganese oxides from soils and rocks. *Eur. J. Soil Sci.* **2004**, *55*, 47–54. [CrossRef]
9. Neaman, A.; Martínez, C.E.; Trolard, F.; Bourrié, G. Trace element associations with Fe- and Mn-oxides in soil nodules: Comparison of selective dissolution with electron probe microanalysis. *Appl. Geochem.* **2008**, *23*, 778–782. [CrossRef]
10. Suda, A.; Makino, T. Functional effects of manganese and iron oxides on the dynamics of trace elements in soils with a special focus on arsenic and cadmium: A review. *Geoderma* **2016**, *270*, 68–75. [CrossRef]
11. Tan, W.F.; Lui, F.; Li, Y.H.; Hu, H.Q.; Huang, Q.Y. Elemental composition and geochemical characteristics of iron-manganese nodules in main soils of China. *Pedosphere* **2006**, *16*, 72–81. [CrossRef]
12. Yu, X.L.; Lu, S.G. Micrometer-scale internal structure and element distribution of Fe-Mn nodules in Quaternary red earth of Eastern China. *J. Soils Sediments* **2016**, *16*, 621–633. [CrossRef]
13. Ji, W.B.; Yang, Z.F.; Yin, A.J.; Lu, Y.Y.; Ying, R.R.; Yang, Q.; Liu, X. Geochemical characteristics of Fe-Mn nodules with different sizes in soils of high geological background areas. *Chin. J. Ecol.* **2021**, *40*, 2289–2301.
14. Ji, W.B.; Yang, Z.F.; Yin, A.J.; Lu, Y.Y.; Ying, R.R.; Yang, Q.; Liu, X.; Li, B.; Duan, Y.R. Formation mechanisms of iron-manganese nodules in soils from high geological background area of central Guangxi. *Chin. J. Ecol.* **2021**, *40*, 2302–2314.
15. Yuan, D. *Modern Karst*; Science Press: Beijing, China, 2016.
16. GB 15618-2018. Soil Environmental Quality Risk Control Standard for Soil Contamination of Agricultural Land. Ministry of Ecology and Environment of the People's Republic of China: Beijing, China, 2018.
17. Wen, Y.; Li, W.; Yang, Z.; Zhuo, X.; Guan, D.-X.; Song, Y.; Guo, C.; Ji, J. Evaluation of various approaches to predict cadmium bioavailability to rice grown in soils with high geochemical background in the karst region, Southwestern China. *Environ. Pollut.* **2020**, *258*, 113645. [CrossRef]
18. Wen, Y.B.; Li, W.; Yang, Z.F.; Zhang, Q.Z.; Ji, J.F. Enrichment and source identification of Cd and other heavy metals in soils with high geochemical background in the karst region, Southwestern China. *Chemosphere* **2020**, *245*, 125620. [CrossRef]
19. Ji, W.B.; Yang, Z.F.; Yu, T.; Yang, Q.; Wen, Y.B.; Wu, T. Potential Ecological Risk Assessment of Heavy Metals in the Fe-Mn Nodules in the Karst Area of Guangxi, Southwest China. *Bull. Environ. Contam. Toxicol.* **2021**, *106*, 51–56. [CrossRef]
20. Ji, W.B.; Lu, Y.Y.; Zhao, C.Y.; Zhang, X.Y.; Wang, H.; Hu, Z.W.; Yu, T.; Wen, Y.B.; Ying, R.R.; Yang, Z.F. Mineral Composition and Environmental Importance of Fe–Mn Nodules in Soils in Karst Areas of Guangxi, China. *Sustainability* **2022**, *14*, 12457. [CrossRef]

21. Ji, W.B.; Ying, R.R.; Yang, Z.F.; Hu, Z.W.; Yang, Q.; Liu, X.; Yu, T.; Wang, L.; Qin, J.X.; Wu, T.S. Arsenic concentration, fraction, and environmental implication in Fe-Mn Nodules in the karst area of Guangxi. *Water* **2022**, *14*, 3021. [CrossRef]
22. Ji, W.B.; Lu, Y.Y.; Yang, M.; Wang, J.; Zhang, X.Y.; Zhao, C.Y.; Xia, B.; Wu, Y.J.; Ying, Y.Y. Geochemical Characteristics of Typical Karst Soil Profiles in Anhui Province, Southeastern China. *Agronomy* **2023**, *13*, 1067. [CrossRef]
23. Yang, Q.; Yang, Z.F.; Filippelli, G.M.; Ji, J.F.; Ji, W.B.; Liu, X.; Wang, L.; Yu, T.; Wu, T.S.; Zhuo, X.S.; et al. Distribution and secondary enrichment of heavy metal elements in karstic soils with high geochemical background in Guangxi, China. *Chem. Geol.* **2021**, *567*, 120081. [CrossRef]
24. Yang, Q.; Yang, Z.F.; Ji, J.F.; Liu, X.; Ji, W.B.; Wang, L. Characteristics of Mineralogy and Heavy Metal Geochemistry in Ferromanganese Nodule Rich Soils with High Geochemical Background from Guigang, Guangxi. *Geoscience* **2021**, *35*, 1450–1458.
25. Gao, T.; Ke, S.; Wang, S.J.; Li, F.B.; Liu, C.S.; Lei, J.; Liao, C.Z.; Wu, F. Contrasting Mg isotopic compositions between Fe-Mn nodules and surrounding soils: Accumulation of light Mg isotopes by Mg–depleted clay minerals and Fe oxides. *Geochim. Cosmochim. Acta* **2018**, *237*, 205–222. [CrossRef]
26. Lin, K.; Yang, Z.F.; Yu, T.; Ji, W.B.; Liu, X.; Li, B.; Wu, Z.L.; Li, X.; Ma, X.D.; Wang, L.; et al. Enrichment mechanisms of Mo in soil in the karst region Guangxi, China. *Ecotoxicol. Environ. Saf.* **2023**, *255*, 114808. [CrossRef]
27. Qian, J.; Fu, W.; Zheng, G.; Deng, B.; Wu, T. Selenium distribution in surface soil layer of karst area of Guangxi and its affecting factors: A case study of Wuming County. *Acta Pedol. Sin.* **2020**, *57*, 1299–1310.
28. China National Environmental Monitoring Centre (CNEMC). *Elemental Background Values of Soils in China*; Environmental Science Press of China: Beijing, China, 1990.
29. DZ/T 0295–2016. Specification of Land Quality Geochemical Assessment. MLR: Dallas, TX, USA, 2016.
30. Fan, T.; Yang, M.; Li, Q.; Zhou, Y.; Xia, F.; Chen, Y.; Yang, L.; Ding, D.; Zhang, S.; Zhang, X.; et al. A new insight into the influencing factors of natural attenuation of chlorinated hydrocarbons contaminated groundwater: A long-term field study of a retired pesticide site. *J. Hazard. Mater.* **2022**, *439*, 129595. [CrossRef] [PubMed]
31. Sun, Z.; Jiang, Y.; Wang, Q.; Owens, P. Fe-Mn nodules in a southern Indiana loess with a fragipan and their soil forming significance. *Geoderma* **2018**, *313*, 92–111. [CrossRef]
32. Palumbo, B.; Bellanca, A.; Neri, R.; Roe, M.J. Trace metal partitioning in Fe-Mn nodules from Sicilian soils, Italy. *Chem. Geol.* **2001**, *173*, 257–269. [CrossRef]
33. Rudnick, R.L.; Gao, S. 4.1-Composition of the continental crust. In *Treatise on Geochemistry*, 2nd ed.; Elsevier: Amsterdam, The Netherlands, 2014; Volume 4, pp. 1–51.
34. Xi, X.H.; Hou, Q.Y.; Yang, Z.F.; Ye, J.Y.; Yu, T.; Xia, X.Q.; Cheng, H.X.; Zhou, G.; Yao, L. Big data based studies of the variation features of Chinese soil's background value versus reference value: A paper written on the occasion of Soil Geochemical Parameters of China's publication. *Ceophysical Geochem. Explor.* **2021**, *45*, 1095–1108. (In Chinese)
35. Hou, Q.Y.; Yang, Z.F.; Yu, T.; Xia, X.Q.; Cheng, H.; Zhou, G. *Soil Geochemical Dataset of China, 16–17*; Geological Publishing House: Beijing, China, 2020.
36. Adriano, D.C. *Trace Elements in the Terrestrial Environment*; Springer Science & Business Media: Berlin/Heidelberg, Germany, 2013.
37. LaForce, M.J.; Fendorf, S.E.; Li, G.C.; Rosenzweig, R.F. Redistribution of trace elements from contaminated sediments of Lake Coeur d'Alene during oxygenation. *J. Environ. Qual.* **1999**, *28*, 1195–1200. [CrossRef]
38. Arachchi, L.; Tokashiki, Y.; Baba, S. Mineralogical characteristics and micromorphological observations of brittle/soft Fe/Mn concretions from Okinawan soils. *Clays Clay Miner.* **2004**, *52*, 462–472. [CrossRef]
39. Liu, F.; Colombo, C.; Adamo, P.; He, J.Z.; Violante, A. Trace elements in manganese–iron nodules from a Chinese Alfisol. *Soil Sci. Soc. Am. J.* **2002**, *66*, 661–670. [CrossRef]
40. Cornu, S.; Deschatrettes, V.; Salvador-Blanes, S.; Clozel, B.; Hardy, M.; Branchut, S.; Forestier, L.L. Trace element accumulation in Mn–Fe–oxide nodules of a planosolic horizon. *Geoderma* **2005**, *125*, 11–24. [CrossRef]
41. Szymański, W.; Skiba, M. Distribution, morphology, and chemical composition of Fe-Mn nodules in albeluvisols of the Carpathian Foothills, Polans. *Pedosphere* **2013**, *23*, 445–454. [CrossRef]
42. Szymański, W.; Skiba, M.; Błachowski, A. Mineralogy of Fe-Mn nodules in Albeluvisols in the Carpathian Foothills, Poland. *Geoderma* **2014**, *217–218*, 102–110. [CrossRef]
43. Timofeeva, Y.O.; Karabtsov, A.A.; Semal, V.A.; Burdukovskii, M.L.; Bondarchuk, N.V. Iron-manganese nodules in Udepts: The dependence of the accumulation of trace elements on nodule size. *Soil Sci. Soc. Am. J.* **2014**, *78*, 767–778. [CrossRef]
44. Feng, Y.F.; Liao, Q.L.; Ji, W.B.; Ren, J.L.; Ji, J.F.; Yang, Z.F.; Zhuo, X.X.; Wang, L.; Liu, Y.Y. Geochemical characteristics of heavy metal enrichment in soil Fe-Mn nodules in the karst area of Guangxi. *Geol. J. China Univ.* **2022**, *28*, 787–798.
45. Feng, X.H.; Zhai, L.M.; Tan, W.F.; Liu, F.; He, J.Z. Adsorption and redox reactions of heavy metals on synthesized Mn oxide minerals. *Environ. Pollut.* **2007**, *147*, 366–373. [CrossRef]
46. Backes, C.A.; McLaren, R.G.; Rate, A.W.; Swift, R.S. Kinetics of cadmium and cobalt desorption from iron and manganese oxides. *Soil Sci. Soc. Am. J.* **1995**, *59*, 778–785. [CrossRef]
47. Tan, W.; Liu, F.; Feng, X.; Huang, Q.; Li, X. Adsorption and redox reactions of heavy metals on the Fe-Mn nodules from Chinese soils. *J. Colloid Interface Sci.* **2005**, *284*, 600–605. [CrossRef]
48. Manceau, A.; Tamura, N.; Marcus, M.A.; MacDowell, A.A.; Celestre, R.S.; Sublett, R.E.; Sposito, G.; Padmore, H.A. Deciphering Ni sequestration in soil ferromanganese nodules by combining X-ray fluorescence, absorption, and diffraction at micrometer scales of resolution. *Am. Miner.* **2002**, *87*, 1494–1499. [CrossRef]

49. Aide, M. Elemental composition of soil nodules from two alfisols on an alluvial terrace in Missouri. *Soil Sci.* **2005**, *170*, 1022–1033. [CrossRef]
50. Manning, B.A.; Fendorf, S.E.; Bostick, B.; Suarez, D.L. Arsenic (III) oxidation and arsenic (V) adsorption reactions on synthetic birnessite. *Environ. Sci. Technol.* **2002**, *36*, 976–981. [CrossRef] [PubMed]
51. Tzou, Y.M.; Wang, M.; Loeppert, R.H. Sorption of phosphate and Cr(VI) by Fe(III) and Cr(III) hydroxides. *Arch. Environ. Contam. Toxicol.* **2003**, *44*, 445–453. [CrossRef]
52. Manceau, A.; Tamura, N.; Celestre, R.S.; MacDowell, A.A.; Geoffroy, N.; Sposito, G.; Padmore, H.A. Molecular-scale speciation of Zn and Ni in soil ferromanganese nodules from loess soils of the Mississippi basin. *Environ. Sci. Technol.* **2003**, *37*, 75–80. [CrossRef] [PubMed]
53. Sipos, P.; Németh, T.; May, Z.; Szalai, Z. Accumulation of trace elements in Fe-rich nodules in a neutral-slightly alkaline floodplain soil. *Carpathian J. Earth Environ. Sci* **2011**, *6*, 13–22.
54. Sipos, P.; Balázs, R.; Bozsó, G.; Németh, T. Changes in micro-fabric and redistribution of Fe and Mn with nodule formation in a floodplain soil. *J. Soils Sediments* **2016**, *16*, 2105–2117. [CrossRef]
55. Šegvić, B.; Girardclos, S.; Zanoni, G.; González, C.A.; Steimer-Herbet, T.; Besse, M. Origin and paleoenvironmental significance of Fe–Mn nodules in the Holocene perialpine sediments of Geneva Basin, western Switzerland. *Appl. Clay Sci.* **2018**, *160*, 22–39. [CrossRef]
56. Ji, H.B.; Wang, S.J.; Ouyang, Z.Y.; Zhang, S.; Sun, C.; Liu, X.; Zhou, D. Geochemistry of red residua underlying dolomites in karst terrains of Yunnan-Guizhou Plateau II. The mobility of rare earth elements during weathering. *Chem. Geol.* **2004**, *203*, 29–50. [CrossRef]
57. Chang, C.; Beckford, H.O.; Ji, H. Indication of Sr Isotopes on Weathering Process of Carbonate Rocks in Karst Area of Southwest China. *Sustainability* **2022**, *14*, 4822. [CrossRef]
58. Li, X.; Han, G.; Liu, M.; Liu, J.; Zhang, Q.; Qu, R. Potassium and its isotope behaviour during chemical weathering in a tropical catchment affected by evaporite dissolution. *Geochim. Cosmochim. Acta* **2022**, *316*, 105–121. [CrossRef]
59. Rambeau, C.M.C.; Baize, D.; Saby, R.; Matera, V.; Adatte, T.; Föllmi, K.B. High cadmium concentrations in Jurassic limestone as the cause for elevated cadmium levels in deriving soils: A case study in Lower Burgundy, France. *Environ. Earth Sci.* **2010**, *61*, 1573–1585. [CrossRef]
60. Langmuir, D. *Aqueous Environmental Geochemistry*; Prentice Hall: Upper Saddle River, NJ, USA, 1997.